Global and Planetary Change 221 (2023) 104024

Contents lists available at ScienceDirect

Global and Planetary Change

journal homepage: www.elsevier.com/locate/gloplacha

Late Quaternary terrigenous sediment supply in the Drake Passage in response to Patagonian and Antarctic ice dynamics

Shuzhuang Wu [a,b,*], Gerhard Kuhn [a], Helge W. Arz [c], Lester Lembke-Jene [a], Ralf Tiedemann [a], Frank Lamy [a], Bernhard Diekmann [d]

[a] Alfred-Wegener-Institut Helmholtz-Zentrum für Meeres- und Polarforschung, 27568 Bremerhaven, Germany
[b] Institute of Earth Sciences, University of Lausanne, 1015 Lausanne, Switzerland
[c] Leibniz Institute for Baltic Sea Research Warnemünde, 18119 Rostock, Germany
[d] Alfred-Wegener-Institut Helmholtz-Zentrum für Meeres- und Polarforschung, 14473 Potsdam, Germany

ARTICLE INFO

Editor: Dr. Fabienne Marret-Davies

Keywords:
Drake Passage
Provenance
Ice sheet dynamics
Sea level changes
Antarctic Circumpolar Current

ABSTRACT

The Drake Passage, as the narrowest passage around Antarctica, exerts significant influences on the physical, chemical, and biological interactions between the Pacific and Atlantic Ocean. Here, we identify terrigenous sediment sources and transport pathways in the Drake Passage region over the past 140 ka BP (thousand years before present), based on grain size, clay mineral assemblages, geochemistry and mass-specific magnetic susceptibility records. Terrigenous sediment supply in the Drake Passage is mainly derived from the southeast Pacific, southern South America and the Antarctic Peninsula. Our results provide robust evidence that the Antarctic Circumpolar Current (ACC) has served as the key driver for sediment dispersal in the Drake Passage. High glacial mass accumulation rates indicate enhanced detrital input, which was closely linked to a large expansion of ice sheets in southern South America and on the Antarctic Peninsula during the glacial maximum, as significantly advanced glaciers eroded more glaciogenic sediments from the continental hinterlands into the Drake Passage. Moreover, lower glacial sea levels exposed large continental shelves, which together with weakened ACC strength likely amplified the efficiency of sediment supply and deposition in the deep ocean. In contrast, significant glaciers' shrinkage during interglacials, together with higher sea-level conditions and storage of sediment in nearby fjords reduced terrigenous sediment inputs. Furthermore, a stronger ACC may have induced winnowing effects and further lowered the mass accumulation rates. Evolution of ice sheets, sea level changes and climate related ACC dynamic have thus exerted critical influences on the terrigenous sediment supply and deposition in the Drake Passage region over the last glacial-interglacial cycle.

1. Introduction

The Drake Passage, located between southern Patagonia and the Antarctic Peninsula, is a ~ 800-km wide oceanic gateway. It is one of the key areas for understanding the interactions of the cryosphere–ocean–atmosphere system during global climate change (Rintoul, 2018; Toggweiler and Samuels, 1995). The mid- and high-latitude atmosphere–ocean dynamic is predominately modulated by the Southern Hemisphere westerly wind belt (SWW) (Lamy et al., 2019; Toggweiler et al., 2006). The SWW acts an essential driver of the Antarctic Circumpolar Current (ACC), which is the world's largest ocean current, flowing eastward through the Drake Passage (Marshall and Speer, 2012; Meredith et al., 2011; Toggweiler and Samuels, 1995). At present, the eastward ACC transports sedimentary material from the South Pacific to the South Atlantic, as traced by clay minerals with chlorite mainly delivered from the Antarctic Peninsula and the Pacific margin of Patagonia as well as reworked smectite from the pelagic South Pacific (Fig. 1) (Biscaye, 1965; Diekmann et al., 2000; Ehrmann et al., 1992; Petschick et al., 1996; Wu et al., 2019). This strong ACC system may have had significant impacts on past spatial distributions of terrigenous sediments in the Southern Ocean (Diekmann et al., 2000; Noble et al., 2012; Walter et al., 2000).

Investigations of variations in terrigenous sources and sedimentation processes over the last glacial cycle have been previously conducted in the Drake Passage region. The SWW was proposed as a major aeolian driver to transport fine sediment from South America to the Scotia Sea,

* Corresponding author at: Alfred-Wegener-Institut Helmholtz-Zentrum für Meeres- und Polarforschung, 27568 Bremerhaven, Germany.
E-mail address: shuzhuangwu@gmail.com (S. Wu).

https://doi.org/10.1016/j.gloplacha.2022.104024
Received 30 June 2022; Received in revised form 19 December 2022; Accepted 20 December 2022
Available online 23 December 2022

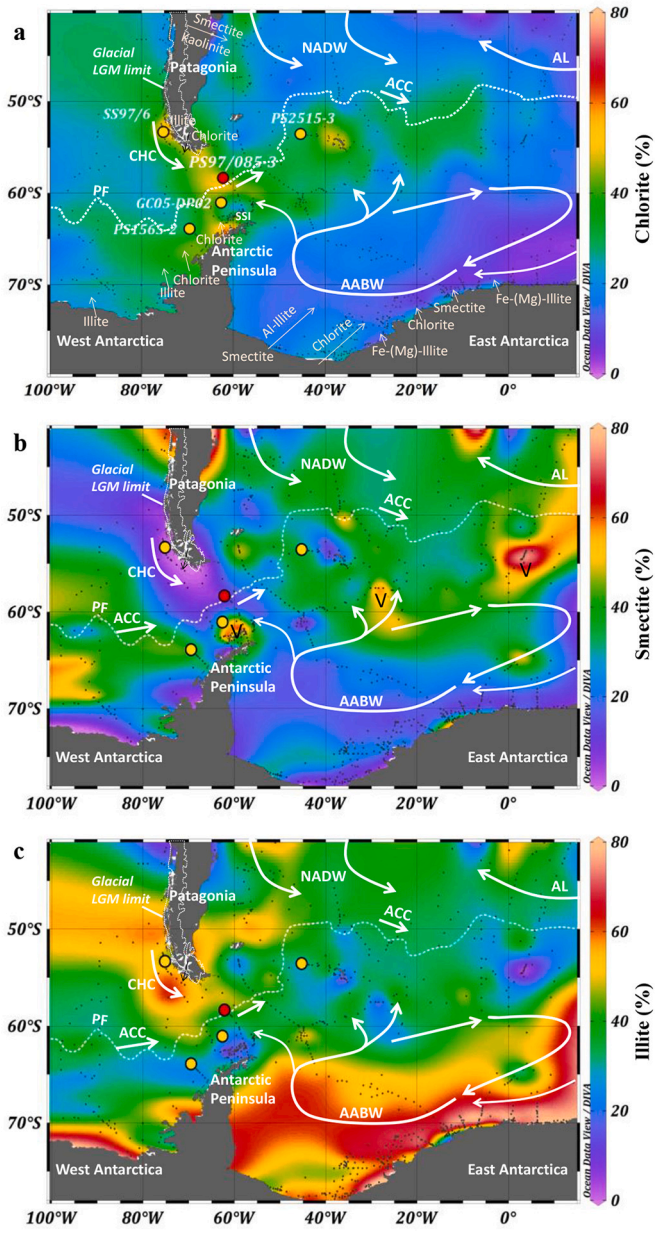

Fig. 1. Clay mineral distributions in the modern Southern Ocean. a Chlorite contents with potential terrigenous sources. b Smectite contents. c Illite contents. Red dot marks the study site PS97/085. Yellow dots show locations of sediment cores from previous studies (Diekmann et al., 2000; Hillenbrand and Ehrmann, 2001; Marinoni et al., 2008; Park et al., 2019). Small black points mark surface samples in study area (see Table 1). The white frame indicates the expansion of the Patagonian ice sheet during the Last Glacial Maximum (LGM) (Davies et al., 2020). White dotted line is Polar Front (PF) (Orsi et al., 1995). V symbols represent volcanic sources. SSI, South Shetland Islands. White arrows indicate potential current transport trajectories. AABW, Antarctic Bottom Water; ACC, Antarctic Circumpolar Current; AL, Agulhas Leakage; CHC, Cape Horn Current; NADW, North Atlantic Deep Water. (For interpretation of the references to colour in this figure legend, the reader is referred to the web version of this article.)

South Atlantic, South Pacific subantarctic zone and Antarctica during the late Pleistocene (Struve et al., 2020; Sugden et al., 2009; Weber et al., 2022; Weber et al., 2012). However, a recent study showed coarser glacial dust grain sizes are recorded in the South Pacific, while finer glacial grain sizes are preserved in the South Atlantic (van der Does et al., 2021). This opposite glacial-interglacial pattern of dust grain-size records in the Pacific and Atlantic sectors of the Southern Ocean is contrary to the long-range dust transport via the circumpolar SWW (Struve et al., 2020). Moreover, mineralogical and geochemical signals from surface sediments and sediment cores records in the Drake Passage region indicate that ocean currents probably played a significant role in dispersal of terrigenous sediments during the glacial periods and the Holocene (Diekmann et al., 2000; Petschick et al., 1996; Walter et al., 2000; Wu et al., 2019). Also, changes in glacier extent and ice sheet variability may have had influences on terrigenous sediment supply in the open ocean (Caniupan et al., 2011; Diekmann et al., 2000; Shin et al., 2020; Weber et al., 2014). The clarification of sources and routes of sediment dispersal in the Southern Ocean has to consider manifold interpretations, invoking dust supply, glacial runoff, as well as erosion of existing shelf and deep-sea sediments (Diekmann et al., 2000; Hillenbrand et al., 2003; Lamy et al., 2014; Petschick et al., 1996; Pugh et al., 2009; Shin et al., 2020; Weber et al., 2014; Weber et al., 2012; Yamazaki and Ikehara, 2012).

In this study, we integrate new and published data of sediment sample sets from the Drake Passage sector of the Southern Ocean (Fig. 1; Table. 1). We aim to identify the specific sources and high-resolution temporal variations in terrigenous sediment supply to the central Drake Passage based on grain size, geochemistry, magnetic properties and clay mineralogy. Specific characteristics in sediment compositions shed light on sediment transport processes and ice dynamics in southern Patagonia and on the Antarctic Peninsula over the last 140 ka.

2. Material and methods

The investigated sediment cores were retrieved from site PS97/085 in the central Drake Passage (58° 21.3′ S, 62° 10.0′ W; water depth 3090 m; Fig. 1). They were taken by piston coring (14.4 m core length) and also comprised material from the trigger core. The study site is located in the northern part of the spreading center of the West Scotia Ridge and on the northern flank of the ridge next to the Shackleton Fracture Zone (Lamy, 2016).

The age model of core PS97/085–3, based on a combination of radiocarbon dates, paleomagnetic excursions, relative paleointensity, and tuning of high-resolution X-ray fluorescence (XRF) scanning-derived ln(Ca/Ti) ratios to Antarctic temperature anomalies, has been published previously (Wu et al., 2021b). Here, we adopted the age model as defined in our previous study without modification. Mass accumulation rates (MAR) were calculated from linear sedimentation rates and dry bulk sediment densities (Wu et al., 2021b).

Core PS97/085–3 was sampled (~ 0.5 cm^3) at 1-cm intervals for grain size measurements. The bulk sediments were treated with hydrogen peroxide (15%) and hydrochloric acid (0.5 mol/l) to remove

Table 1
Clay mineral composition of sediment samples in the Drake Passage region.

Samples	Latitude	Longitude	Water depth (m)	References
SS97–6	53° 19.1′ S	75° 12.0′ W	1896	Marinoni et al. (2008)
PS2515–1	53° 33.4′ S	45° 18.6′ W	3522	Diekmann et al. (2000)
PS97/085–3	58° 21.3′ S	62° 10.0′ W	3091	This study
GC05-DP02	61° 2.70′ S	62° 38.4′ W	3503	Park et al. (2019)
PS1565–2	63° 54.5′ S	69° 30.5′ W	3427	Hillenbrand and Ehrmann (2001)
Surface samples (no. 722)	78° S ~ 48° S	100° W ~ 15° E	0~7906	Biscaye (1965); Wu et al. (2019); Ehrmann et al. (1992); Petschick et al. (1996); Diekmann and Kuhn (1999); Hillenbrand et al. (2003).

the organic matter and the carbonates, respectively. Biogenic opal content, sampled every 10 cm, was measured with a leaching method (151 samples, maximum at 5.1%, mean 2.2%) on bulk sediment and because of its low concentration not needed to be removed. Subtracting the (pore water salt corrected) biogenic opal, total organic carbon and carbonate content (both measured with element analyzers) from total sediment (100%) results in terrigenous fraction (Wu et al., 2021b). Grain-size of the terrigenous fractions were measured with a CILAS 1180 laser diffraction particle-size analyzer at the Alfred Wegener Institute Helmholtz Centre for Polar and Marine Research (AWI), List/Sylt (Wu et al., 2021b).

High-resolution logging of the magnetic volume susceptibility (κMS_{bulk}) on core PS97/085–3 was performed with a Bartington MS2E sensor in combination with an MS2 control unit, integrated into a fully automated split-core logger. Magnetic susceptibility was obtained every 1 mm directly on the split surface of the cores (Wu et al., 2021b). To obtain the variations in composition of the pure terrigenous material, without dilution by pore water or biogenic contents (carbonate and biogenic opal), we calculated the mass-specific magnetic susceptibility of the terrigenous fraction (χMS_{terr}), following established routines (Dearing, 1994; Diekmann et al., 2000).

The major elemental composition was measured with an AVAATECH XRF core scanner at AWI, Bremerhaven. Measurement settings have been reported previously (Wu et al., 2021b). Five major elements intensities (Al, Si, Fe, Ti and Ca) were retrieved from 10 kV measurements to discuss terrigenous sediment supply in this study. Samples for clay mineral analyses (<2 μm sediment fraction) were taken at 4-cm intervals and the fine fraction (<63 μm) was separated by the Atterberg method into silt (2–63 μm) and clay (<2 μm). Measurements on clay fraction were carried out by X-ray diffractometry (XRD) using a Malvern Panalytical Empyrean goniometer (40 kV, 40 mA, Cu-Kα radiation) on glycolated preferentially oriented mounts. We used the MacDiff software for semi-quantitative estimates of peak areas of the basal reflection for the main clay mineral groups (smectite at 17 Å, illite at 10 Å, and chlorite at 7 Å) (Petschick et al., 1996). The 5 Å/10 Å peak intensity ratios were used to provide illite crystallinity conditions. High intensity ratios (>0.4) correspond to Al-rich illite while low intensity ratios (<0.25) indicate Fe—Mg rich illite (Esquevin, 1969; Petschick et al., 1996). The relative number of Fe atoms in octahedral sites of chlorite were calculated by the relative intensities of the chlorite 00 *l* series (002, 003 and 004 reflections). Fe-rich chlorite is mainly produced by hydrothermally altered ferromagnesian minerals of basic igneous and metamorphic rocks (Deer et al., 2013; Lamy et al., 1998). Further analytical details for clay mineralogy have been reported previously (Petschick et al., 1996; Wu et al., 2019).

We performed a principal component analysis (PCA) on the following 16 terrigenous related variables: contents of smectite, illite, chlorite, Fe-rich chlorite, quart/feldspar ratio, χMS_{terr}, ice rafted debris (IRD), percentage of lithogenic composition, contents of sand, silt and clay, Fe/Ca and Ti/Ca, Fe/Al, Ti/Al and Si/Al. Prior to the application of the PCA, all datasets were resampled at 1 ka resolution. All data were standardized to unit variance using their individual mean and standard deviation. PCA was performed using the built-in functions in the Python pca package (Taskesen, 2020). The SPE/DmodX (distance to model) was used to detect outliners based on the mean and covariance of the first two principal components (Taskesen, 2020).

3. Results

The terrigenous sediment fractions of core PS97/085–3 is dominated by silt and sand, while the clay fraction is a minor component (Fig. 2a). The silt fraction yields maximum content, varying between 42% and 89%, with an average of 77%. The sand fraction ranges from 0 to 54%, with an average of 15%, while the clay fraction ranges from 3% to 18%, with an average of 8% (Fig. 2a). High sand contents prevailed during Marine Isotope Stage (MIS) 5 and MIS 1 interglacials, while the silt and clay fractions featured higher percentages during the full glacials. Elevated abundances of IRD occurred during the glacial periods, reaching the maximum during MIS 6 (Fig. 2b). The IRD contents at our site are generally lower than 2 vol% except for a peak of 18 vol% during late MIS 4 (Wu et al., 2021b). Higher mass accumulation rates prevailed during the glacial periods (20–50 g cm^{-2} ka^{-1}) and lower ones during interglacials (<10 g cm^{-2} ka^{-1}, Fig. 2c).

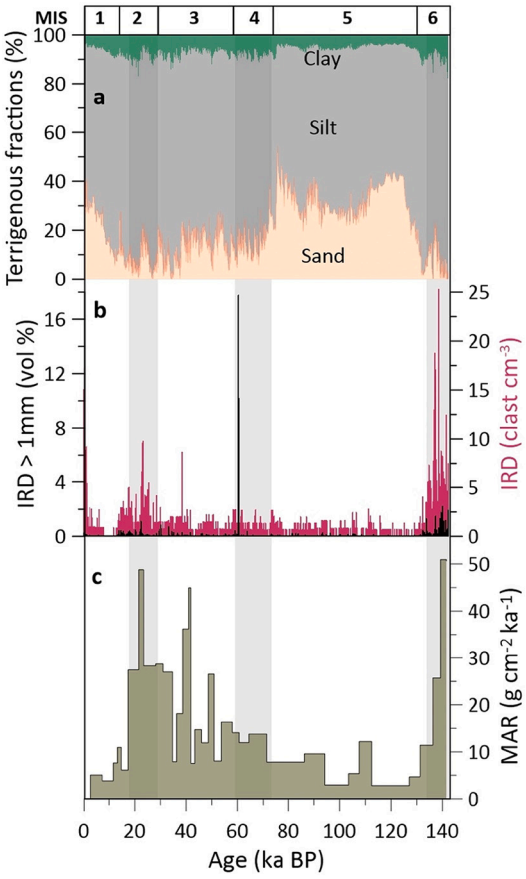

Fig. 2. a Terrigenous grain size compositions of core PS97/085–3. b Ice rafted debris volume percentage (IRD > 1 mm, black) and IRD clast numbers cm^{-3} (pink) in core PS97/085–3 (Wu et al., 2021b). c Mass accumulation rates (MAR). MIS, Marine Isotope Stage (Lisiecki and Raymo, 2005). (For interpretation of the references to colour in this figure legend, the reader is referred to the web version of this article.)

In marine sediments, Ti and Fe contents are primarily related to lithogenic materials, while Ca mostly documents variations in calcium carbonate concentrations (maximum 36% during interglacials and minimum 0.3% during glacials; 6.4% on average) (Wu et al., 2021b). Past changes in Ti/Ca and Fe/Ca ratios can thus be applied to reflect variations in detrital input (Arz et al., 1998; Govin et al., 2012). Moreover, Si and Ti are enriched in coarse siliciclastic sediment components, while Al mainly relates to fine-grained clay minerals in the sediment (Biscaye, 1965). Si/Al and Ti/Al have been used to represent grain size changes (Govin et al., 2012; Lamy et al., 2015). Higher Si/Al and Ti/Al ratios prevail during MIS 5 and the Holocene (Fig. 3a, b). In contrast, low Fe/Ca and Ti/Ca ratios are present during interglacial periods and increase to their maximum values during MIS 6 and 2 (Fig. 3c, d). The χMS_{terr} ranges between 1500 and 3500 $\times$ 10^{-9} m^3 kg^{-1}, which is controlled by the concentration of ferrimagnetic minerals, mainly magnetite (Dearing, 1994). Changes in χMS_{terr} are comparable to the variations of Fe/Ca and Ti/Ca ratios, with the longest lasting and highest values ~3500 $\times$ 10^{-9} m^3 kg^{-1} of χMS_{terr} during MIS 6 and 2, and short maxima at about 120 ka and 79 ka, and the lowest short lasting values at about 132 ka, 85 ka, and longer lasting lower values below 2000 $\times$ 10^{-9}

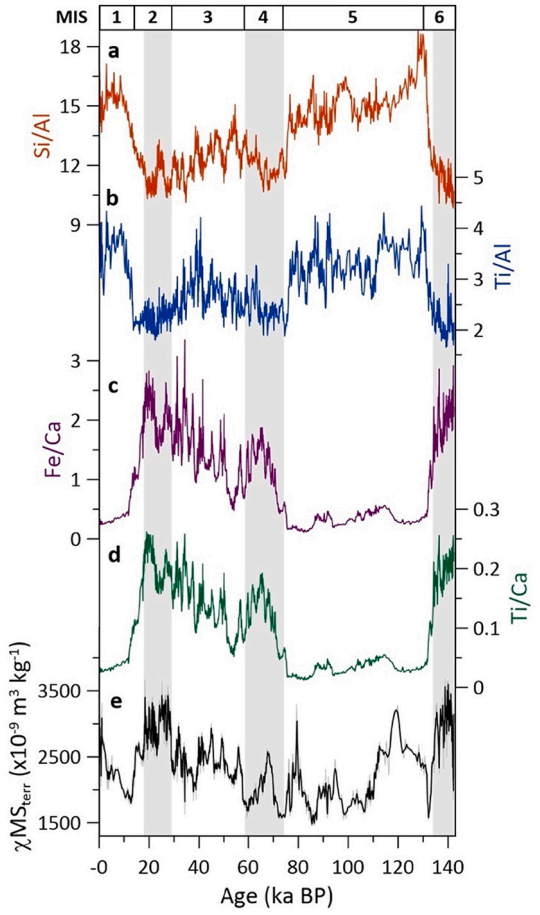

Fig. 3. Bulk element ratios and magnetic property (bulk sediment) of core PS97/085–3. a, b Changes in Si/Al and Ti/Al ratios. c, d Changes in Fe/Ca and Ti/Ca ratios. e Variations in mass-specific magnetic susceptibility (χMS_{terr}, black). Grey bars indicate the glacial periods.

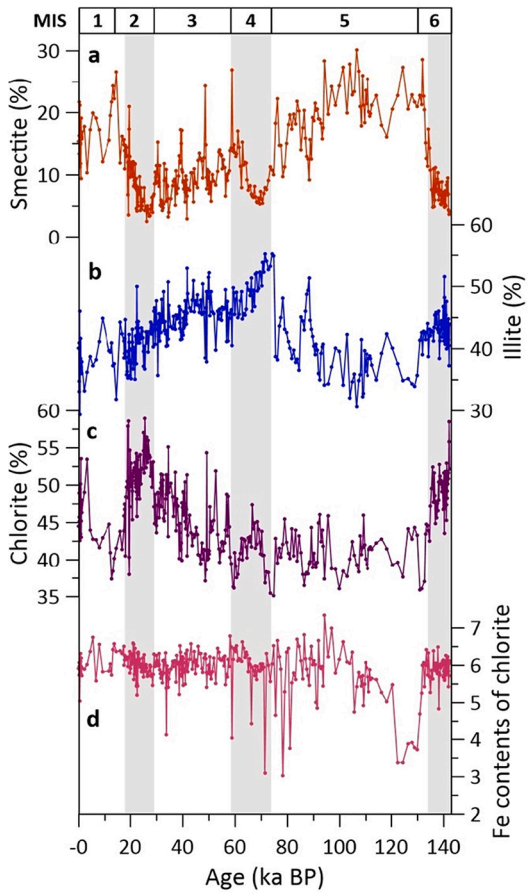

Fig. 4. Clay mineral contents (<2 μm fraction) and magnetic property (bulk sediment) of core PS97/085–3. a Smectite contents with three-point smoothing (red curve). b Illite contents with three-point smoothing (blue curve). c Chlorite contents with three-point smoothing (purple curve). d The variation of relative number of Fe-atoms in the octahedral positions of chlorite (pink curve). Grey bars indicate the glacial periods. (For interpretation of the references to colour in this figure legend, the reader is referred to the web version of this article.)

$m^3\ kg^{-1}$ between 108 and 96 ka, 75 to 72 ka, 64 to 58 ka and 13 to 9 ka (Fig. 3c-e). Compared to the MIS 6 and 2, relatively low χMS_{terr} values are shown during MIS 4, with an average of 2040 × 10^{-9} $m^3\ kg^{-1}$. Characteristic millennial-scale fluctuations with small magnitudes in χMS_{terr} occur during MIS 3 (Fig. 3e).

The clay minerals in the clay fraction (<2 μm) in the terrigenous sediments of core PS97/085–3 are mainly composed of illite (29–58%) and chlorite (32–59%), while the amount of smectite is relatively low to intermediate (2–30%) (Fig. 4a-c). Kaolinite was below the limit of detection in all samples at our site. The glacial periods are characterized by low smectite contents (2–10%) associated with low amplitude variability. Chlorite (42–59%) and illite (34–58%) contents present high values and their fluctuations show a reverse pattern in comparison to changes in smectite contents (Fig. 4a-c). The relative abundance of smectite increased abruptly from ~5 to 28% during deglaciations and remains at high values (20–30%) during interglacials, while the chlorite and illite contents decreased to their minimums (~30%). The amount of illite increased abruptly from MIS 5 (~30%) to its maximum (58%) during MIS 4 and subsequently decreased to MIS 2 (Fig. 4b). The 5 Å/10 Å ratios of illite are generally higher than 0.4, suggesting Al-rich illite with a good crystallinity was dominant over the past 140 ka. In contrast, relative constant low chlorite abundances with an average of 40% prevail during MIS 5 and then increase >20% from MIS 4 to MIS 2 (Fig. 4c). Specifically, the total Fe contents of chlorite is lower during MIS 4 than during MIS 6 and 2 (Fig. 4d).

The PCA analysis classified two distinct principal components (PCs), which account for ~65% of the total variance of the data matrix (Fig. 5). The first principal component (PC1) captures the maximum variance (~53%) of the data and clearly characterizes the variations of terrigenous sediment supply quantities in the Drake Passage. The second principal component (PC2) accounts for ~12% of the total variance and is mainly controlled by χMS_{terr} value and illite content. Other PCs explain individually for <10% of the remaining variance.

4. Discussion

4.1. Sediment provenance in the Drake Passage

Our records exhibit pronounced glacial-interglacial fluctuations over the past 140 ka. Since the clay mineral assemblages reveal distinct temporal changes, we applied the ratios of smectite/(chlorite + illite) and quartz/feldspar to describe the mineralogical variations within the clay fraction (Fig. 6).

During the full glacial stages MIS 6 and 2 (Jouzel et al., 1989), we find low smectite/(chlorite + illite), quartz/feldspar, Ti/Al, and Si/Al ratios associated with high χMS_{terr} values, and Fe-rich chlorite, Ti/Ca and Fe/Ca ratios (Figs. 3, 4 and 6). These features are consistent with basic to intermediate and undifferentiated parent rocks in the southern South America and on the Antarctic Peninsula (Burton-Johnson and Riley, 2015; Diekmann et al., 2000; Hillenbrand et al., 2009; Marinoni et al., 2008). Detritus from metamorphic and basic lithologies generally contains large amounts of magnetite minerals, which result in high

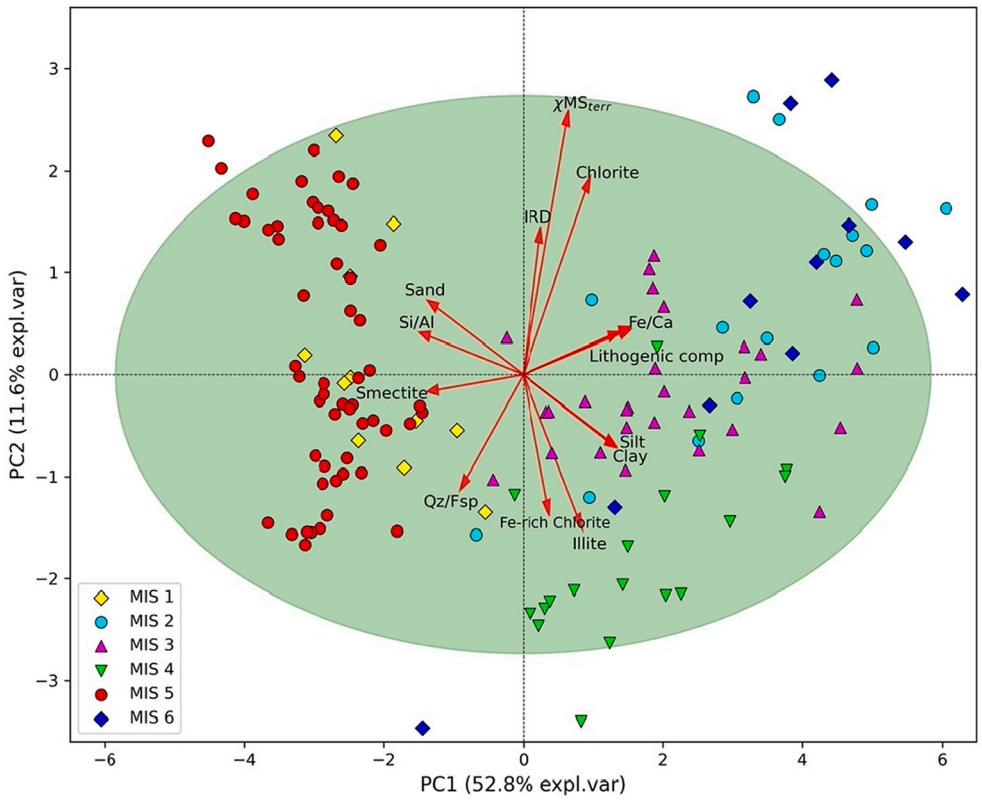

Fig. 5. Principal component analysis results with 95% confidence ellipse. Biplot of the PC1 and PC2 explains ~65% of the total variance with input data projections on the principal components. The parameters of the biplot are directly related to terrigenous sediment supply quantities and provenance. The length of the arrows representing a known variable is a function of its importance in determining the parameters' variation.

χMS_{terr}, Ti/Ca and Fe/Ca ratios (Dearing, 1994; Diekmann et al., 2000). These glacial sequences are rich in illite and chlorite and are associated with low smectite contents (Diekmann et al., 2000; Hillenbrand et al., 2009; Marinoni et al., 2008; Wu et al., 2019). The variations of smectite/(chlorite + illite) and quartz/feldspar ratios in the central Drake Passage (core PS97/085–3) are broadly consistent with the clay mineral spectrum and χMS_{terr} values in the northern Scotia Sea (core PS2515–3; Figs. 6-7) (Diekmann et al., 2000). These two records, together with a record from the Antarctic Peninsula continental margin (core PS1565–2) (Hillenbrand and Ehrmann, 2001), show low smectite/(chlorite + illite) ratios during glacial periods, indicative of high sediment input from southern South America and the Antarctic Peninsula (Fig. 6). This suggestion is supported by similar glacial clay mineral assemblages pattern in cores close at the Chilean Margin, i.e., core SS97–6 (Marinoni et al., 2008) and off the Antarctic Peninsula i.e., core GC05-DP02 (Park et al., 2019). The smectite contents in the southern sites are relatively higher (>20% in cores PS1565–2 and GC05-DP02; Fig. 7b) than those in the northern records (<20% in cores PS97/085–3, PS2515–3 and SS97–6). We attribute this gradient to the respective distances from the smectite source, since several volcanoes developed at the Antarctic Peninsula on the South Shetland Islands, which together with hydrolytic conditions may potentially be a source for smectite (Diekmann et al., 2000; Hillenbrand and Ehrmann, 2001; Park et al., 2019; Petschick et al., 1996; Wu et al., 2019). Therefore, we suggest that the terrigenous sediments in the central Drake Passage during the full glacial stages were mainly derived from southern South America and the Antarctic Peninsula.

Compared to the full glacial stages MIS 6 and 2, the detrital sediments during MIS 4 are characterized by the highest contents of illite (~60%), relatively low χMS_{terr} values (2040×10^{-9} m^3 kg^{-1}) and low Fe-rich chlorite contents (Figs. 3-4). Such characteristic terrigenous sediment may primarily originate from basic to acidic rocks along the southernmost Chilean Margin and partial adjacent hinterland (Marinoni et al., 2008; Wu et al., 2019). High χMS_{terr} values with an average of 3000×10^{-9} m^3 kg^{-1} and Fe-rich chlorite contents from the Antarctic Peninsula (Diekmann et al., 2000; Wu et al., 2019) therefore can be ruled out as a major source during MIS 4. We suggest that enhanced detritus supply from the Antarctic Peninsula to the central Drake Passage probably started from MIS 4 to MIS 2 coeval to the increase in χMS_{terr} and Fe-rich chlorite (Figs. 3-4).

In contrast to the glacial stages, we found high smectite/(chlorite + illite), quartz/feldspar, Si/Al and Ti/Al ratios with low χMS_{terr} values during the glacial-interglacial transitions, MIS 5, 3 and 1 (Figs. 3, 4 and 6). These sediment composition features might have been caused by reworked older sediments from the Chilean Margin and southeast Pacific (Figs. 3, 4 and 6). Relatively high smectite contents (27–46%) were reported in reworked sediments from the southeast Pacific (Diekmann et al., 2003) and high quartz/feldspar ratios have been found along the Chilean Margin in the surface samples and sediment cores during interglacials (Marinoni et al., 2000; Marinoni et al., 2008; Wu et al., 2019). Smectite-rich sediments might have been contributed to the high smectite contents at the Antarctic Peninsula, especially around the volcanic South Shetland Islands (over 90% smectite) (Park et al., 2019; Petschick et al., 1996; Wu et al., 2019). However, low χMS_{terr} values occurred during the interglacials, against high χMS_{terr} values in the Antarctic Peninsula source (Diekmann et al., 2000). A strong ACC during interglacials (Lamy et al., 2015; Toyos et al., 2020; Wu et al., 2021b) likely caused higher amounts of reworking of fine-grained sediments and transported from the southeast Pacific into the central Drake Passage, which is supported by consistent signatures in the downstream area of the Drake Passage (Diekmann et al., 2000; Noble et al., 2012; Walter et al., 2000). Moreover, the eastward flow of the ACC would prevent input of smectite from the Atlantic-side of Patagonia (Diekmann et al., 2000; Marinoni et al., 2000). Therefore, we suggest that during interglacials, detrital sediments in the central Drake Passage were

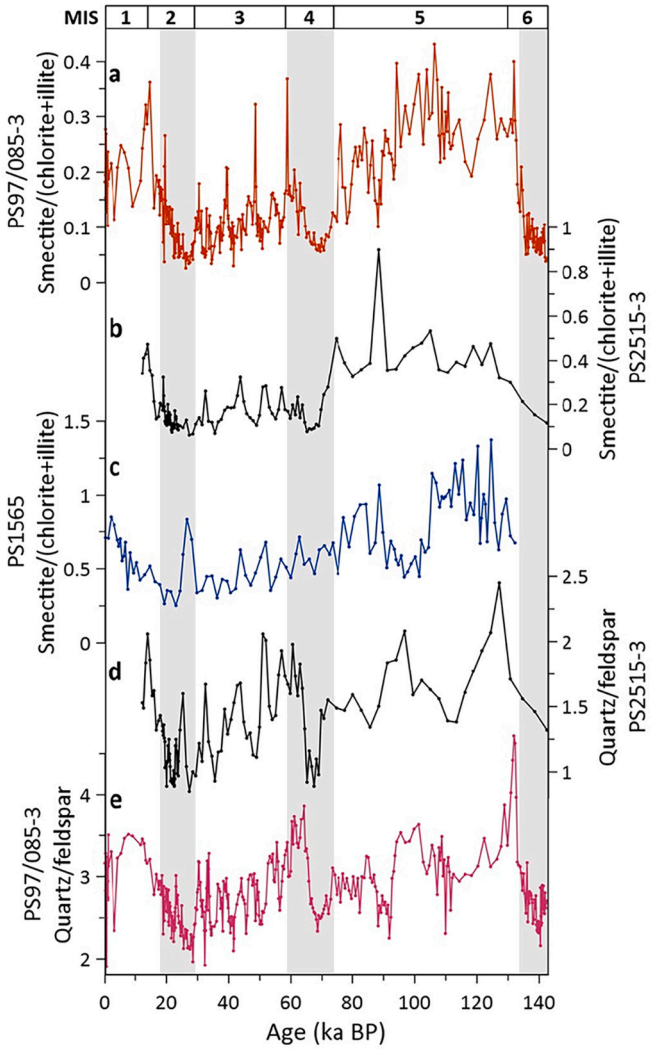

Fig. 6. Comparison of past changes in clay mineralogy records in the Drake Passage region over the last 140 ka. a, b, c Smectite/(chlorite + illite) ratios in cores PS97/085–3 (red, this study), PS2515–3 (black; Diekmann et al., 2000) and PS1565 (blue; Hillenbrand and Ehrmann, 2001), respectively. d, e Quartz/feldspar ratios in cores PS2515–3 (black; Diekmann et al., 2000) and PS97/085–3 (pink, this study). Grey bars indicate the glacial periods. (For interpretation of the references to colour in this figure legend, the reader is referred to the web version of this article.)

mainly derived from the pelagic southeast Pacific (Fig. 7a). Smectite/(chlorite + illite), quartz/feldspar ratios and χMS_{terr} exhibit medium values during MIS 3, oscillating between glacial and interglacial conditions. This suggests the Drake Passage might have received sediment input from different sources, i.e., alternating from the southern Chilean Margin, the pelagic southeast Pacific and the Antarctic Peninsula sources (Figs. 5 and 7a).

4.2. Impact of transport mechanisms on source signals

Although estimates of past changes in ACC strength differ between studies depending on the respective site locations (Lamy et al., 2015; McCave et al., 2014; Roberts et al., 2017; Toyos et al., 2020), our recent study from the same sediment core reveals a stronger ACC during interglacials in the central Drake Passage compared to glacial stages (Fig. 8e) (Wu et al., 2021b). A strong ACC during interglacials would have increased sediment winnowing (e.g., PC1 shows negative values during MIS 5 and the Holocene. Fig. 8d), resulting in high smectite/(chlorite + illite) ratios and lower the mass accumulation rates. Expansion of the ice sheets in southern Patagonia and on the Antarctic Peninsula associated with glacial sea level low-stands would enhance terrigenous inputs, which have reached our site through hemipelagic transport processes. A slowdown of the ACC (including the Cape Horn Current) during glacials has been recorded in the Chilean Margin and the Drake Passage (Lamy et al., 2015; Toyos et al., 2020; Wu et al., 2021b), allowing for enhanced settling and deposition of fine-grained sediments and increased the mass accumulation rates (Figs. 2-3). Therefore, the strong ACC changes between glacial and interglacials played an important role for sediment transport and deposition in the central Drake Passage over the past 140 ka.

Aeolian supply may act as a potential additional transport mechanism to deliver terrigenous sediment to our study area. Strong SWW have been suggested as an important driver for dust supply during glacials (Lamy et al., 2014; Sugden et al., 2009; Weber et al., 2022; Weber et al., 2012). However, high crystallinity, Al-rich illite and a lack of detectable kaolinite at our site exclude the possibility of significant aeolian transport from Patagonian dust, which is rather characterized by kaolinite and Fe-Mg-rich illite with poor crystallinity (Camilión, 1993; Diekmann et al., 2000; Ito and Wagai, 2017; Petschick et al., 1996). Moreover, high glacial χMS_{terr} values (~3500 × 10^{-9} m^3 kg^{-1}) in our record is much higher than the average values (100–500 × 10^{-9} m^3 kg^{-1}) found in Pampa loesses (Orgeira et al., 1998). Evidence from clay mineral assemblages, magnetic and geochemical properties of bulk glacial sediments in the Drake Passage and southeastern Pacific region do not support significant aeolian transport to the Drake Passage area over the last glacial either (Diekmann et al., 2000; Noble et al., 2012; Shin et al., 2020; Walter et al., 2000; Wengler et al., 2019). Moreover, a recent study highlighted the non-aeolian terrigenous input from South America rather than aeolian transport in the Pacific entrance to the Drake Passage (Toyos et al., 2022).

Besides aeolian supply, turbidity currents might be important for sediment dispersal on continental slopes and abyssal plains (Barker and Burrell, 1977; Campbell and Clark, 1977). Since our site is located close to the crest of the ridge next to the Shackleton Fracture Zone (Lamy, 2016), turbidity currents likely only had a minor, or no effect on sedimentation there. For ice-rafting transport, our record shows higher IRD contents during the peak glacials, which might contribute to higher χMS_{terr}. Often the size fraction >154 μm is used as an IRD proxy as well (Wu et al., 2021a), but our grain size distribution curves clearly show that especially with high bottom current velocities during interglacials the fine sand grain sizes up to 250 μm are current sorted (see Wu et al., 2021b, Suppl. Fig. 4) and could not be used as an IRD indicator for this site. Here, we used the size fraction >1 mm as an IRD proxy, which are generally <2 vol% at our site (Wu et al., 2021b) and its fluctuation shows virtually no similarity to the χMS_{terr} curves (Figs. 2-3), thus ice-rafted transport can hence be excluded as a significant source of sediment transport in the central Drake Passage. Because at this site even the fine sand can be current sorted (Wu et al., 2021b), we cannot rule out that some of these particles were primarily brought by ice but overprinted by current sorting. There is some correlation of the mass% >125 μm and the χMS_{terr} curve during MIS 1 and MIS 5 specially the maxima at early MIS 5 and late MIS 5. Since sea ice in the Antarctic region only carries material from dust (Weber et al., 2012), sea-ice transport thus have a negligible impact in the central Drake Passage. Overall, we suggest that the ACC exerted a predominant role in sediment dispersal to the Drake Passage, affecting past changes in terrigenous proxy records.

4.3. Linking the terrigenous sediment inputs to Patagonian and Antarctic Peninsula ice sheets dynamics

The reconstructed variability of terrigenous sediment supply into the Drake Passage exhibits glacial-interglacial fluctuations of sediment erosion and transport in response to the waxing and waning of the Patagonian and the Antarctic Peninsula ice sheets, falling and rising of

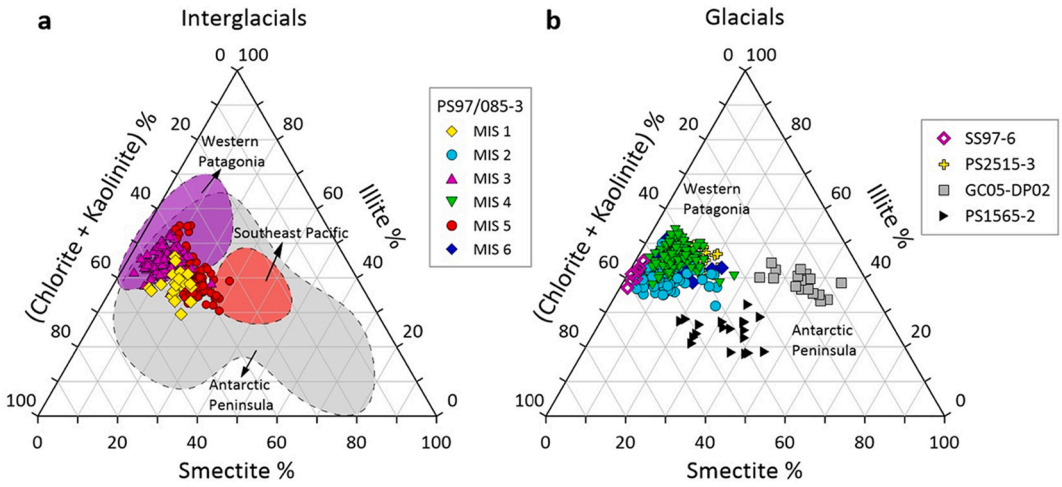

Fig. 7. Potential provenance sources based on the clay mineral assemblages. a Ternary diagram of smectite-illite-(chlorite + kaolinite) during interglacials. The warm stages (MIS 1, 3 and 5) are marked by yellow diamonds, violet up-triangles and red dots, respectively. Purple shapes represent modern western Patagonia sediment source. Grey shapes represent the Antarctic Peninsula source. Red shapes represent Southeast Pacific source. These sources are defined by clay mineral assemblages from published surface samples and core tops in the study area (Biscaye, 1965; Diekmann and Kuhn, 1999; Diekmann et al., 2000; Ehrmann et al., 1992; Hillenbrand and Ehrmann, 2001; Marinoni et al., 2000; Park et al., 2019; Petschick et al., 1996; Wu et al., 2019). b Potential terrigenous sources during glacials. Clay mineral assemblages during MIS 2, 4 and 6 in core PS97/085–3 are marked by cyan dots, green down-triangles and blue diamonds, respectively. (For interpretation of the references to colour in this figure legend, the reader is referred to the web version of this article.)

sea level and changes in ocean current strength over the past 140 ka (Fig. 8). The ice sheets in southern Patagonia and on the Antarctic Peninsula reached their maximum extents during MIS 6 and 2 (Davies et al., 2020; EPICA Community Members, 2006; Kaplan et al., 2005; Moreno et al., 2015; Sugden et al., 2009), which have significantly increased the glacial erosion and thus increased terrigenous sediment supply from the continental hinterlands to the Drake Passage (i.e., PC1 and PC2 show more positive values). Moreover, variations in PC1 clearly follows past changes in sea level during the last glacial cycle (Fig. 8b, d) (Rohling et al., 2014). We suggest that low eustatic sea level stands during full glaciations led to subaerial exposure of large continental shelf regions around South America and ice covered large continental shelf region around Antarctica, which would further amplify the erosion efficiency and increase the sediment flux into the deep ocean (Fig. 8).

A distinct pattern for the full glacial stages MIS 6 and 2 deviates from MIS 4 (Fig. 8). Detrital sediments in the Drake Passage were mainly derived from the Chilean continental margin and its partial hinterland during MIS 4. At this interval, at least the northwestern margin of the Patagonian ice-sheet, had prevailing wet-based and faster flowing ice streams, which significantly increased the glacial erosion as precipitation was high compared to Antarctica (Kaiser and Lamy, 2010; Lamy et al., 2004; Peltier et al., 2021). Furthermore, past instability of the Patagonian ice sheet may have led to enhanced meltwater plumes, which would have fed terrigenous sediments into the Drake Passage (Cowan et al., 2008; Diekmann et al., 2000; Marinoni et al., 2008; Pudsey, 2000). Rapid glacier advance has been reconstructed in southern Patagonia during MIS 4 (Mendelová et al., 2020; Sugden et al., 2009). A recent study reported the southern Patagonian ice sheet was more extensive during MIS 4 than during MIS 2 (Peltier et al., 2021). This ice sheet expansion may have contributed to a spike of IRD content in our records (Fig. 2b). However, the ice sheets may not have reached into the open ocean during MIS 4 (Mendelová et al., 2020; Peltier et al., 2021; Sugden et al., 2009). Moderate terrigenous sediment supply might have been attributed to most of detritus becoming trapped in proximal Chilean fjords at this interval (Fig. 8).

Sequentially, our records show increases in χMS_{terr} values and chlorite (Fig. 3e and 4c) as well as PC1 and PC2 loadings from MIS 4 to MIS 2 (Fig. 8), indicative of a gradual shift in the terrigenous sources at times of ice sheet expansion. The glacial expansion of the Patagonian and the Antarctic Peninsula ice sheets towards the open ocean and the accompanying drops in sea level would activate the large continental shelf areas as an additional source of sediment erosion (Kilian and Lamy, 2012; Rohling et al., 2014; Sugden et al., 2009). Therefore, we ascribe the glacial maxima in terrigenous sediment supply to the central Drake Passage primarily to the advancement of Patagonia and Antarctic Peninsula glaciers, combined with the exposure of large continental shelf regions during sea level low-stands. This is supported by decreased smectite/(chlorite + illite) ratios in our Drake Passage sediment record as well as at the southern Chilean Margin (Marinoni et al., 2008), the northern Scotia Sea (Diekmann et al., 2000) and the Antarctic Peninsula (Hillenbrand and Ehrmann, 2001; Park et al., 2019) during glacial expansions.

The deglacial periods are marked by a significant retreat of glaciers and increasing relative sea levels (Davies et al., 2020; Kilian and Lamy, 2012; Rohling et al., 2014; Sugden et al., 2009). As the ACC transported more heat towards higher latitudes (Hillenbrand et al., 2017; Weber et al., 2014), significant meltwater plumes are especially expected at the glacial terminations in response to periods of rapid melting. However, the χMS_{terr} values are marked by deglacial decreases indicative of a reduced terrigenous sediment input across the glacial terminations consistent also with the Chilean Margin records further north (Kaiser and Lamy, 2010). The short-lived spikes in smectite/(chlorite + illite) and quartz/feldspar ratios (Fig. 6) yielded in negative PC2 loadings during the glacial terminations and might be an expression of more mature sediment deposition during rapid ice sheets retreat and meltwater-related changes from the Patagonia and Antarctic Peninsula (Fig. 8). The short χMS_{terr} maxima and positive PC2 loadings at early MIS 5 and 1(Fig. 8f-g), close to peak warm interglacial, could perhaps result by IRD input and therefore higher Antarctic and Patagonian hinterland supply similar to glacials of the fine sand fraction redistributed by currents. The last χMS_{terr} minima at 13 to 9 ka (early MIS 1) just followed the Antarctic Cold Reversal (Graham et al., 2017) and may be related to a period of higher summer sea surface temperature records south of the Polar Front (Bianchi and Gersonde, 2004) and perhaps more precipitation and meltwater runoff.

5. Conclusions

High-resolution grain size and clay mineral assemblages together with geochemical and magnetic properties reveal significant changes in

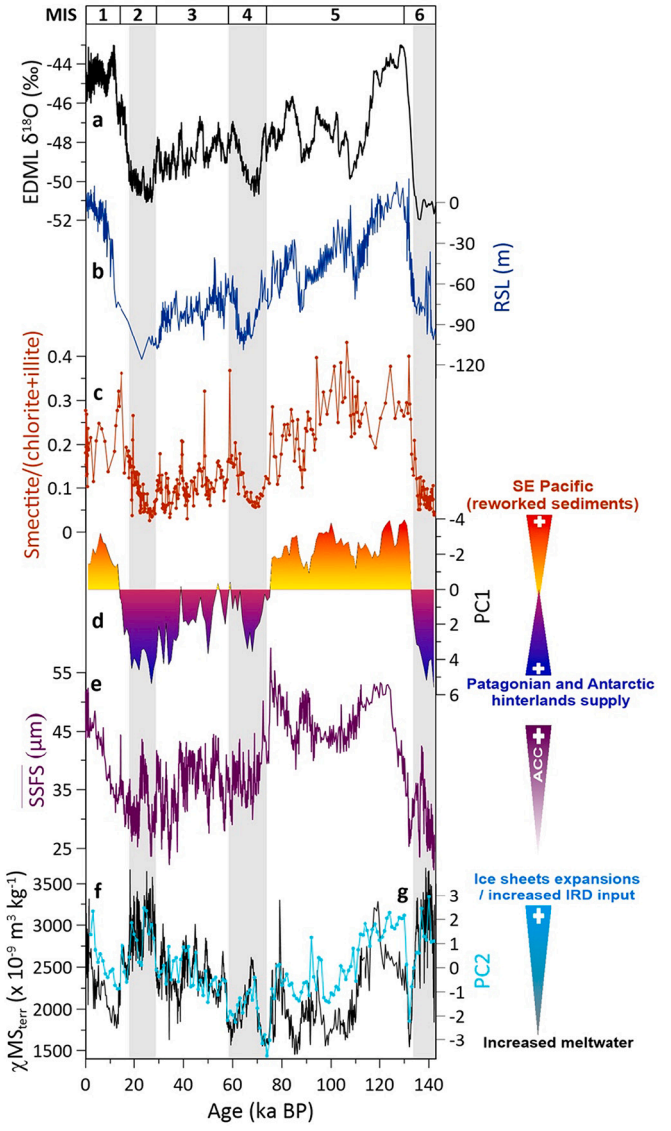

Fig. 8. The variability of terrigenous supply compared to changes in ice dynamics, sea level and current strength. a Oxygen isotope records from the EPICA Dronning Maud Land (EDML) ice core can be a proxy as ice volume (EPICA Community Members, 2006). b Relative sea level (Rohling et al., 2014). c Smectite/(chlorite + illite) ratios. d PC1 loadings derived from the PCA (reversed scale). Positive values indicate Patagonian and Antarctic Peninsula ice sheets expansions increased terrigenous supply from the continental hinterlands, while negative values reflect ice sheets retreat reduced detrital input and strong ACC induced and transported reworked sediments from the southeast Pacific. e Mean sortable silt plus fine sand ($\overline{SSFS}$) from the same core PS97/085–3 as a flow-speed proxy for the ACC strength (Wu et al., 2021b). f Mass-specific magnetic susceptibility record. g PC2 loadings derived from the PCA. Positive values indicate ice sheet expansions or increased IRD input, while negative ones imply increased meltwater runoff.

the amount and provenance of terrigenous sediment supply in the central Drake Passage over the past 140 ka. Our records reveal that the detrital sediment fraction is mainly derived from the southeast Pacific, southern South America and the Antarctic Peninsula. Significant aeolian transport can be ruled out in the Drake Passage, based on the clear assignment of the regional provenance of terrigenous material. The ACC (including the Cape Horn Current) had likely served as the major driver for lateral sediment transport in the Drake Passage region during the last glacial-interglacial cycle. Increased current speeds during interglacials have been likely responsible for reworking of sediment from the southeast Pacific into the Drake Passage. In contrast, expansion of ice sheets in southern Patagonia and on the Antarctic Peninsula combined with relative sea-level low-stands and weakened current speeds led to enhance the efficiency of terrigenous input and deposition during glacial maxima. Furthermore, our continuous high-resolution marine records provide complementary evidence for ice sheet advancement and if combined with comparable more ice proximal records better sediment provenance reconstruction from the onset of glaciation towards the glacial maximum, which is often not resolved by fragmentary terrestrial records.

Declaration of Competing Interest

The authors declare no conflicts of interests to this work.

Data availability

Datasets in this article are available online on PANGAEA Data Publisher for Earth & Environmental Science. https://doi.pangaea.de/10.1594/PANGAEA.933043.

Acknowledgements

We acknowledge Rita Fröhlking-Teichert, Susanne Wiebe and Valea Schumacher at AWI for technical assistance in sample preparation and analytical measurements. We thank Y. K. Park for the clay mineral dataset from core GC05-DP02. We thank N. Nowaczyk, X. Zhang, X. Zheng and S. Jaccard for helpful discussions. This work has been supported by the AWI research programmes (Changing Earth–Sustaining our Future and PACES-II grants) and China Scholarship Council and Deutsche Forschungsgemeinschaft (WU 1062 1-1).

References

Arz, H.W., Pätzold, J., Wefer, G., 1998. Correlated millennial-scale changes in surface hydrography and terrigenous sediment yield inferred from last-glacial marine deposits off Northeastern Brazil. Quat. Res. 50 (2), 157–166.
Barker, P., Burrell, J., 1977. The opening of Drake passage. Mar. Geol. 25 (1-3), 15–34.
Bianchi, C., Gersonde, R., 2004. Climate evolution at the last deglaciation: the role of the Southern Ocean. Earth Planet. Sci. Lett. 228 (3-4), 407–424.
Biscaye, P.E., 1965. Mineralogy and sedimentation of recent deep-sea clay in the Atlantic Ocean and adjacent seas and oceans. Geol. Soc. Am. Bull. 76 (7), 803–832.
Burton-Johnson, A., Riley, T., 2015. Autochthonous v. accreted terrane development of continental margins: a revised in situ tectonic history of the Antarctic Peninsula. J. Geol. Soc. 172 (6), 822–835.
Camilión, M.C., 1993. Clay mineral composition of pampean loess (Argentina). Quat. Int. 17, 27–31.
Campbell, J.S., Clark, D.L., 1977. Pleistocene turbidites of the Canada abyssal plain of the Arctic Ocean. J. Sediment. Res. 47 (2), 657–670.
Caniupan, M., et al., 2011. Millennial-scale sea surface temperature and Patagonian Ice Sheet changes off southernmost Chile (53 degrees S) over the past similar to 60 kyr. Paleoceanography 26.
Cowan, E.A., Hillenbrand, C.-D., Hassler, L.E., Ake, M.T., 2008. Coarse-grained terrigenous sediment deposition on continental rise drifts: a record of Plio-Pleistocene glaciation on the Antarctic Peninsula. Palaeogeogr. Palaeoclimatol. Palaeoecol. 265 (3), 275–291.
Davies, B.J., et al., 2020. The evolution of the Patagonian Ice Sheet from 35 ka to the present day (PATICE). Earth Sci. Rev. 204, 103152.
Dearing, J.A., 1994. Environmental Magnetic Susceptibility: Using the Bartington MS2 System.
Deer, W.A., Howie, R.A., Zussman, J., 2013. An Introduction to the Rock-Forming Minerals. Mineralogical Society of Great Britain and Ireland.
Diekmann, B., Kuhn, G., 1999. Provenance and dispersal of glacial–marine surface sediments in the Weddell Sea and adjoining areas, Antarctica: ice-rafting versus current transport. Mar. Geol. 158 (1), 209–231.
Diekmann, B., et al., 2000. Terrigenous sediment supply in the Scotia Sea (Southern Ocean): response to Late Quaternary ice dynamics in Patagonia and on the Antarctic Peninsula. Palaeogeogr. Palaeoclimatol. Palaeoecol. 162 (3-4), 357–387.
Diekmann, B., et al., 2003. Terrigenous Sediment Supply in the Polar to Temperate South Atlantic: Land-Ocean Links of Environmental Changes during the Late Quaternary, The South Atlantic in the Late Quaternary. Springer, Berlin, pp. 375–399.
Ehrmann, W.U., Melles, M., Kuhn, G., Grobe, H., 1992. Significance of clay mineral assemblages in the Antarctic Ocean. Mar. Geol. 107 (4), 249–273.
EPICA Community Members, 2006. One-to-one coupling of glacial climate variability in Greenland and Antarctica. Nature 444 (7116), 195–198.

Esquevin, J., 1969. Influence de la composition chimique des illites sur leur cristallinité. Bull. Centre Rech. Pau-SNPA 3 (1), 147–153.
Govin, A., et al., 2012. Distribution of major elements in Atlantic surface sediments (36°N–49°S): imprint of terrigenous input and continental weathering. Geochem. Geophys. Geosyst. 13 (1).
Graham, A.G., et al., 2017. Major advance of South Georgia glaciers during the Antarctic Cold Reversal following extensive sub-Antarctic glaciation. Nat. Commun. 8, 14798.
Hillenbrand, C.D., et al., 2017. West Antarctic Ice Sheet retreat driven by Holocene warm water incursions. Nature 547 (7661), 43–48.
Hillenbrand, C.D., Ehrmann, W., 2001. Distribution of clay minerals in drift sediments on the continental rise west of the Antarctic Peninsula, ODP Leg 178, Sites 1095 and 1096. In: Barker, P., Camerlenghi, A., Acton, G.D., Ramsay, A.T.S. (Eds.), Proc. ODP, Sci. Results, p. 178.
Hillenbrand, C.D., Grobe, H., Diekmann, B., Kuhn, G., Fütterer, D.K., 2003. Distribution of clay minerals and proxies for productivity in surface sediments of the Bellingshausen and Amundsen seas (West Antarctica)–Relation to modern environmental conditions. Mar. Geol. 193 (3), 253–271.
Hillenbrand, C.D., et al., 2009. Clay mineral provenance of sediments in the southern Bellingshausen Sea reveals drainage changes of the West Antarctic Ice Sheet during the Late Quaternary. Mar. Geol. 265 (1), 1–18.
Ito, A., Wagai, R., 2017. Global distribution of clay-size minerals on land surface for biogeochemical and climatological studies. Sci. Data 4, 170103.
Jouzel, J., et al., 1989. Global change over the last climatic cycle from the vostok ice core record (Antarctica). Quat. Int. 2, 15–24.
Kaiser, J., Lamy, F., 2010. Links between Patagonian Ice Sheet fluctuations and Antarctic dust variability during the last glacial period (MIS 4-2). Quat. Sci. Rev. 29 (11), 1464–1471.
Kaplan, M.R., Douglass, D.C., Singer, B.S., Ackert, R.P., Caffee, M.W., 2005. Cosmogenic nuclide chronology of pre-last glacial maximum moraines at Lago Buenos Aires, 46°S, Argentina. Quat. Res. 63 (3), 301–315.
Kilian, R., Lamy, F., 2012. A review of Glacial and Holocene paleoclimate records from southernmost Patagonia (49–55°S). Quat. Sci. Rev. 53, 1–23.
Lamy, F., 2016. The expedition PS97 of the research vessel POLARSTERN to the Drake Passage in 2016. Berichte zur Polar-und Meeresforschung Rep. Polar Mar. Res. 701.
Lamy, F., Hebbeln, D., Wefer, G., 1998. Terrigenous sediment supply along the Chilean continental margin: modern regional patterns of texture and composition. Geol. Rundsch. 87 (3), 477–494.
Lamy, F., et al., 2004. Antarctic timing of surface water changes off Chile and Patagonian ice sheet response. Science 304 (5679), 1959–1962.
Lamy, F., et al., 2014. Increased dust deposition in the Pacific Southern Ocean during glacial periods. Science 343 (6169), 403–407.
Lamy, F., et al., 2015. Glacial reduction and millennial-scale variations in Drake Passage throughflow. Proc. Natl. Acad. Sci. 112 (44), 13496–13501.
Lamy, F., et al., 2019. Precession modulation of the South Pacific westerly wind belt over the past million years. Proc. Natl. Acad. Sci. 201905847.
Lisiecki, L.E., Raymo, M.E., 2005. A Pliocene-Pleistocene stack of 57 globally distributed benthic δ18O records. Paleoceanography 20 (1), PA1003.
Marinoni, L., Setti, M., Gauthier-Lafaye, F., 2000. Surface carbonate and land-derived clastic marine sediments from southern Chile: mineralogical and geochemical investigation. J. S. Am. Earth Sci. 13 (8), 775–784.
Marinoni, L., Setti, M., Salvi, C., Lopez-Galindo, A., 2008. Clay minerals in late Quaternary sediments from the south Chilean margin as indicators of provenance and palaeoclimate. Clay Miner. 43 (2), 235–253.
Marshall, J., Speer, K., 2012. Closure of the meridional overturning circulation through Southern Ocean upwelling. Nat. Geosci. 5, 171–180.
McCave, I., Crowhurst, S., Kuhn, G., Hillenbrand, C., Meredith, M., 2014. Minimal change in Antarctic Circumpolar Current flow speed between the last glacial and Holocene. Nat. Geosci. 7 (2), 113–116.
Mendelová, M., Hein, A.S., Rodés, Á., Xu, S., 2020. Extensive mountain glaciation in central Patagonia during Marine Isotope Stage 5. Quat. Sci. Rev. 227, 105996.
Meredith, M.P., et al., 2011. Sustained monitoring of the Southern Ocean at Drake Passage: past achievements and future priorities. Rev. Geophys. 49 (4).
Moreno, P.I., et al., 2015. Radiocarbon chronology of the last glacial maximum and its termination in northwestern Patagonia. Quat. Sci. Rev. 122, 233–249.
Noble, T.L., et al., 2012. Greater supply of Patagonian-sourced detritus and transport by the ACC to the Atlantic sector of the Southern Ocean during the last glacial period. Earth Planet. Sci. Lett. 317, 374–385.
Orgeira, M.J., et al., 1998. Mineral magnetic record of paleoclimate variation in loess and paleosol from the Buenos Aires formation (Buenos Aires, Argentina). J. S. Am. Earth Sci. 11 (6), 561–570.
Orsi, A.H., Whitworth III, T., Nowlin Jr., W.D., 1995. On the meridional extent and fronts of the Antarctic Circumpolar Current. Deep-Sea Res. I Oceanogr. Res. Pap. 42 (5), 641–673.
Park, Y.K., et al., 2019. Elemental compositions of smectites reveal detailed sediment provenance changes during glacial and interglacial periods: the Southern Drake Passage and Bellingshausen Sea, Antarctica. Minerals 9 (5), 322.
Peltier, C., et al., 2021. The large MIS 4 and long MIS 2 glacier maxima on the southern tip of South America. Quat. Sci. Rev. 262, 106858.
Petschick, R., Kuhn, G., Gingele, F., 1996. Clay mineral distribution in surface sediments of the South Atlantic: sources, transport, and relation to oceanography. Mar. Geol. 130 (3), 203–229.
Pudsey, C.J., 2000. Sedimentation on the continental rise west of the Antarctic Peninsula over the last three glacial cycles. Mar. Geol. 167 (3), 313–338.
Pugh, R., McCave, I., Hillenbrand, C.-D., Kuhn, G., 2009. Circum-Antarctic age modelling of Quaternary marine cores under the Antarctic Circumpolar Current: ice-core dust–magnetic correlation. Earth Planet. Sci. Lett. 284 (1-2), 113–123.
Rintoul, S.R., 2018. The global influence of localized dynamics in the Southern Ocean. Nature 558 (7709), 209–218.
Roberts, J., et al., 2017. Deglacial changes in flow and frontal structure through the Drake Passage. Earth Planet. Sci. Lett. 474, 397–408.
Rohling, E.J., et al., 2014. Sea-level and deep-sea-temperature variability over the past 5.3 million years. Nature 508 (7497), 477–482.
Shin, J.Y., et al., 2020. Particle-size dependent magnetic properties of Scotia Sea sediments since the Last Glacial Maximum: glacial ice-sheet discharge controlling magnetic proxies. Palaeogeogr. Palaeoclimatol. Palaeoecol. 557, 109906.
Struve, T., et al., 2020. A circumpolar dust conveyor in the glacial Southern Ocean. Nat. Commun. 11 (1), 5655.
Sugden, D.E., McCulloch, R.D., Bory, A.J.-M., Hein, A.S., 2009. Influence of Patagonian glaciers on Antarctic dust deposition during the last glacial period. Nat. Geosci. 2 (4), 281–285.
Taskesen, E., 2020. PCA is a Python Package that Performs the Principal Component Analysis and makes Insightful Plots. (0.1.8). Zenodo.
Toggweiler, J.R., Samuels, B., 1995. Effect of Drake Passage on the global thermohaline circulation. Deep-Sea Res. Part I-Oceanogr. Res. Pap. 42 (4), 477–500.
Toggweiler, J.R., Russell, J.L., Carson, S.R., 2006. Midlatitude westerlies, atmospheric CO2, and climate change during the ice ages. Paleoceanography 21 (2).
Toyos, M.H., et al., 2020. Antarctic Circumpolar Current dynamics at the Pacific entrance to the Drake Passage over the past 1.3 million years. Paleoceanogr. Paleoclimatol. 35 (7) e2019PA003773.
Toyos, M.H., et al., 2022. Variations in export production, lithogenic sediment transport and iron fertilization in the Pacific sector of the Drake Passage over the past 400 ka. Clim. Past Discuss. 2021, 1–37.
van der Does, M., et al., 2021. Opposite dust grain-size patterns in the Pacific and Atlantic sectors of the Southern Ocean during the last 260,000 years. Quat. Sci. Rev. 263, 106978.
Walter, H., Hegner, E., Diekmann, B., Kuhn, G., 2000. Provenance and transport of terrigenous sediment in the South Atlantic Ocean and their relations to glacial and interglacial cycles: Nd and Sr isotopic evidence. Geochim. Cosmochim. Acta 64 (22), 3813–3827.
Weber, M.E., et al., 2012. Dust transport from Patagonia to Antarctica – A new stratigraphic approach from the Scotia Sea and its implications for the last glacial cycle. Quat. Sci. Rev. 36, 177–188.
Weber, M.E, et al., 2014. Millennial-scale variability in Antarctic ice-sheet discharge during the last deglaciation. Nature 510 (7503), 134.
Weber, M.E., et al., 2022. Antiphased dust deposition and productivity in the Antarctic Zone over 1.5 million years. Nat. Commun. 13 (1), 2044.
Wengler, M., et al., 2019. A geochemical approach to reconstruct modern dust fluxes and sources to the South Pacific. Geochim. Cosmochim. Acta 264, 205–223.
Wu, L., et al., 2021a. Late Quaternary dynamics of the Lambert Glacier-Amery Ice Shelf system, East Antarctica. Quat. Sci. Rev. 252, 106738.
Wu, S., et al., 2021b. Orbital- and millennial-scale Antarctic Circumpolar Current variability in Drake Passage over the past 140,000 years. Nat. Commun. 12 (1), 3948.
Wu, S., et al., 2019. Surface sediment characteristics related to provenance and ocean circulation in the Drake Passage sector of the Southern Ocean. Deep-Sea Res. I Oceanogr. Res. Pap. 154, 103135.
Yamazaki, T., Ikehara, M., 2012. Origin of magnetic mineral concentration variation in the Southern Ocean. Paleoceanography 27 (2).